DASINYA JOURNAL for engineering and informatics

https://doi.org/10.65542/djei.v1i1.7
Dasinya Journal for Engineering and Informatics. **2025**, *1*, *1*.

Article

Finite Element Modelling and Experimental Validation of CFRP-Strengthened Reinforced Concrete Beams

Yaman Al-Kamaki [1,*], Riadh Al-Mahaidi [2], Mand Kamal Askar [1] and Razaq Ferhadi [3]

[1] Highway and Bridge Department, Technical College of Engineering, Duhok Polytechnic University (DPU), Duhok 42001, Iraq.
[2] School of Engineering, Swinburne University of Technology, Hawthorn, Australia.
[3] College of Engineering, The American University of Kurdistan (AUK), Duhok, Kurdistan Region, Iraq.
* Correspondence: yaman.alkamaki@dpu.edu.krd

Abstract

Extreme loading and harsh environmental exposure are two of the many variables that can lead to reinforced concrete (RC) beam deterioration. Nowadays, the recommended technique for extending the life duration of degraded structures is the use of fiber-reinforced polymer (FRP) strengthening materials. FRP composites have been utilized to strengthen concrete members since the late 1970s in order to increase their ductility and load-bearing capability. Although FRP has been effectively utilized to repair concrete beams that have deteriorated due to both internal and external influences, the use of appropriate software limits the numerical modeling of Carbon Fiber-Reinforced Polymer (CFRP) for RC beam strengthening. To investigate the structural response, FEMs were developed in ATENA-GiD, aiming to clarify the behavior of both the control beams and those repaired with CFRP, and to assess their load-bearing capacity. This is a unique software that can be used only for RC elements. It can be stated from the experimental results taken from previously published work that the load-bearing capacity and deflection for the control beam were 47.7 kN and 35.7 mm, respectively. By adding one unidirectional CFRP sheet as U-wraps, the load increased and deflection decreased by 24.9 % and 48.2 %, respectively. When using the same test results for verification using FE software, the load-bearing capacity and deflection for the simulated model were 49.4 kN and 37.6 mm, respectively. When adding the CFRP sheet to the model, similar to that of experimental work done. After the analysis stage, the load increased and deflection decreased by 24.1 % and 52.1 %, respectively. This indicates that FRP has become a powerful composite material for strengthening existing RC structures.

Keywords: reinforced concrete (RC) beams; Carbon fiber-reinforced polymer (CFRP); finite element models (FEMs); Strengthening; ATENA-GiD software.

1. Introduction

Many times, reinforced concrete structural elements, due to various reasons, get damaged [1, 2]. In most of the situations, damage appears in the form of concrete spalling, cracks, element fracture, and deflection, etc [3]. Many causes may be responsible for these degenerations, such as thermal damage, overload, rust of steel, earthquake, environmental effects, and accidental impact on the structure [4]. The maintenance process techniques could be economical and fast in processing time. After a structure gets damaged or needs to be retrofitted for higher load carrying or a different purpose of use, structural elements would be weak, and they need to be strengthened [4].

Received: August 28, 2025; Revised: August 31, 2025; Accepted: August 31, 2025; Published: October 12, 2025; Available online: October 12, 2025.

At the end of the 80's of the last century, for the first time, FRP was used in Japan for the purpose of strengthening the structural elements [5]. Due to its high tensile strength, low weight, durability, corrosion resistance, and ease of installation, externally bonded FRP has become a novel structural strengthening technique.

The FRP is categorized by high-strength fibers embedded in polymer resin. The utmost common type of FRP in industry is made with carbon (CFRP), aramid (AFRP), basalt (BFRP), and glass (GFRP). Now, FRP materials have been widely used to increase the shear capacity and flexural strength of RC members [6].

As a robust computational technique, the finite element method (FEM) permits for systematic analysis of the nonlinear response of RC structures [7]. Through FEM, the behavior of structures can be investigated before and after loading, particularly with respect to load–deflection characteristics and crack formation [8, 9]. Furthermore, the outcomes of FEM models must be assessed by contrasting them with full-scale beam experiments. However, the number of test specimens needed to solve a particular problem can be decreased by developing trustworthy analytical models; identifying and carrying out those tests is expensive and time-consuming, and they frequently do not accurately replicate the loading and support conditions of the real structure [10].

The conventional analysis of structural members and systems generally relies on moment distribution, slope-deflection, and matrix methods. For members with complex geometries, these methods either demand simplifications of structural properties or result in tedious analytical procedures, albeit still possible [11].

When compared to reinforced systems, the finite element analysis (FEA) of steel structures and steel members is less complex. The FEA of RC members is extremely challenging due to the following variables [12].

1- The material nown as concrete is not homogeneous. It is quite difficult to describe its behavior in a straightforward mathematical formula. distinct loading types, including monotonic increasing and cyclic loadings, as well as distinct states of stress combinations that may have resulted from different loading systems, cause material properties to differ in directions and from point to point;

2- The behavior of the steel-concrete contact is a complicated three-dimensional phenomenon that is not well understood;

3- There is a lack of clarity on the behavior of concrete and the force transfer across a cracked part once the cracks are developed.

Even though there was a lack of data regarding material behavior and challenges with RC members' FEA, numerous researchers and analysts were able to create models that accurately depicted or replicated every activity and conducted thorough analyses of the members or systems.

One of the first significant applications of the FEM to RC structures was presented by Ngo and Scordelis [13]. In their work, bond–slip effects were represented through the use of dedicated bond-link elements between the concrete and reinforcing steel, and linear elastic analyses of pre-cracked RC beams were conducted. The drawback of this linear elastic formulation, however, was its inability to capture the full nonlinear response of RC members across the entire loading range. Nilson 1968 [14] addressed this shortcoming by introducing nonlinear material models together with nonlinear bond–slip relationships in the analysis of RC beams. At that time, the computational process required the load to be paused at the end of each increment so that updated data could be supplied to the program. With later advancements in nonlinear finite element techniques, this iterative stop–and–update procedure was rendered unnecessary.

Numerous research documenting the behavior of virgin beams externally reinforced with FRP to increase their load-carrying capability can be found in the literature. According to the aforementioned research, externally bonded FRP systems can be utilized to improve the strength and stiffness of reinforced concrete beams while preserving a suitable degree of deformability.

Duthinh and Starnes 2001 [15] experimentally investigated the use of CFRP sheets for the flexural strengthening of RC beams. Their results confirmed the effectiveness of CFRP in enhancing flexural capacity, although the degree of improvement was found to decrease with higher levels of internal steel reinforcement. Building on this, Yang et al. 2003 [16] applied finite element analysis to study the failure associated with concrete cover separation in FRP-plated RC beams subjected to tension. Using a discrete crack model, they demonstrated that the cover separation failure mechanism could be realistically reproduced. Their simulations also indicated that bonding an FRP plate produced more frequent and finer cracks compared to unstrengthened beams, with significant implications for the stress distribution within the plate. Similarly, Supaviriyakit et al. 2004 [17] conducted nonlinear finite element modeling of

RC beams externally strengthened with FRP plates. Their findings exhibited that the numerical models could reliably capture load–deflection behavior, load-carrying capacity, and failure modes, aligning well with experimental evidence.

Santhakumar et al., 2004 [18] used CFRP composites to conduct the analysis of the modified RC shear beams. The behavior of retrofitted RC shear beams was simulated numerically in this study. This numerical modeling aids in tracking the creation and spread of cracks, particularly in retrofitted beams where the wrapping of CFRP composites obscures the fracture patterns for experimental analysis. Ferracuti et al., 2006 [19] examined the FRP-concrete delamination numerical modeling. The delamination phenomenon is studied using a non-linear bond-slip model. This study demonstrated that FRP retrofit may be highly beneficial for enhancing the RC structure's performance under both temporary and permanent service loads. Gao et al. 2007 [20] address the various failure modes of the FRP-strengthened RC beams, such as (i) FRP strip rupture; (ii) compression failure following steel yielding; (iii) compression failure before steel yielding; (iv) FRP strip delamination resulting from a crack; and (v) separation of the concrete cover. After comparing numerous different literatures, the study's findings reveal that epoxy bonding the FRP matrix to the tension stiffness of RC beams can significantly increase the stiffness and ultimate flexural strength.

As a result, a considerable body of research has emerged, involving both experimental and analytical studies on the utilization of composite materials for strengthening and retrofitting structural elements. The growing interest in retrofitting is largely due to its potential to enable early damage recognition and to provide warnings of critical conditions. Researchers have investigated not only the failure mechanisms of FRP-strengthened members but also diverse strengthening strategies employing different FRP materials.

The FE of the RC beam that has been upgraded with FRP is the focus of this study. Previous studies have thoroughly examined the usage of CFRP sheets for retrofitting and reinforcing RC structures. Nonetheless, a great deal of experimental and analytical study has been done on beam strengthening, but little work has been done on the field of precisely retrofitted structural elements. For this reason, the modified beam may be modeled and analyzed using ATENA. Additionally, ATENA-GiD aids in meshing the surface beam and FE modeling. It aids in modeling the deformed beam by providing the load deflection curve, stress-strain values, beam crack width, and beam material at each stage.

2. Materials and Methods

2.1 ATENA-GiD

The research deals with "FE Modeling of the retrofitted and non-retrofitted RC beams" with the help of ATENA-GiD software [21, 22]. ATENA-GiD is limited to RC elements and can be thought of as having two modules. An FEM analysis application called ATENA (Advanced Tool for Engineering Nonlinear Analysis) connects with GiD, a pre- and post-processor program that can do static analysis and create pertinent input and FE meshes. GiD allows ATENA to execute a variety of computation options, such as variable loading and time inputs, through AtenaStudio, an ATENA interface module within GiD. At every point throughout the loading process, loads, displacements, and cracks within the RC beam can be obtained using the ATENA-GiD program. The following sections provide a detailed description of the software's application.

To compare the performance of FRP-retrofitted beams with that of the control beam, the study initially developed FE models of the beams for analysis. Owing to symmetry, four simply supported half-beams were modeled. Among these, one beam was designated as the control specimen, while another was retrofitted with a CFRP sheet. The control beam was first modeled and analyzed using ATENA-GiD, which provided results including the ultimate load and deflection, load–deflection response, stress–strain relationships, and crack development at different stages. Following this, the retrofitted beam was modeled using the control beam's ultimate load and deflection as a reference. An RC beam with discretely modeled steel reinforcement was also developed, and the numerical results were compared with the experimental data stated by Hawileh et al. (2013) [23]. The experimental load–deflection curve was further compared with the analytical predictions to calibrate the FE model for subsequent analyses.

2.2 Modelling RC Beams

RC members are composed of concrete, a heterogeneous material, and steel, which is relatively homogeneous. Although modeling such elements can be challenging, advanced FEM techniques, assuming concrete as a homogeneous

matrix with uniform mechanical properties, can provide valuable insights into their structural behavior. In this study, the non-linear FEM software ATENA-GiD [22] was employed to model the tested beams.

The RC beam tested by Hawileh et al., 2013 [23], shown in Figure 1, was modeled in three dimensions using ATENA-GiD. Owing to the symmetry of both the geometry and the applied load, only half of the beam was modeled. Two scenarios were simulated as follows:

- A control RC beam without CFRP strengthening;
- An RC beam strengthened with a single unidirectional CFRP sheet bonded to its exterior surface.

2.3 Pre-Processing

GiD provides a user-friendly platform for defining beam geometry, assigning material properties, applying boundary conditions, and specifying the loading history. It automatically generates the interval data and corresponding finite element meshes required for static analysis. The analysis results produced in ATENAStudio can then be imported back into GiD, which also functions as an effective post-processor for visualization. Before carrying out a nonlinear finite element analysis in ATENAStudio, the structural model must be fully prepared in GiD, including the geometry, material definitions, such as the CFRP wrapping—boundary conditions, and meshing.

2.3.1 Geometrical Model

The geometry of a typical RC beam is illustrated in Figure 1, with experimental dimensions and load–deflection results adopted from Hawileh et al. 2013 [23]. To reduce computation time, only half of the beam was modeled, with boundary conditions applied to satisfy symmetry requirements. For the unwrapped beam, the model consisted of three main elements; when CFRP sheets were applied, a fourth element was added. The steel reinforcement, including longitudinal bars and stirrups, was represented using 1-D elements, whereas CFRP sheets were modeled as thin shell elements. Concrete and steel end plates were represented as 3-D solid elements. The beam assembly in GiD included half of the RC beam volume, with steel plates positioned at the top and bottom surfaces, and reinforcing steel introduced as line entities. Full contact was assumed between the concrete's top and bottom surfaces and the adjacent steel plates. Thin elastic shell elements were assigned to represent the CFRP layers, while an interface element was introduced between the inner surface of the CFRP and the external beam surface to account for imperfect bonding. The final FE model geometry, including all components and meshing, is presented in Figure 2.

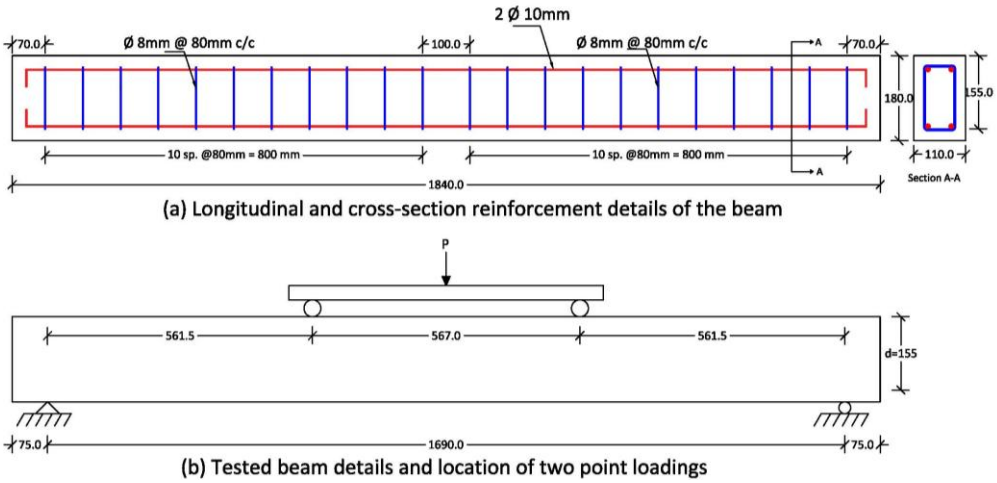

Figure 1. Geometry of RC beam tested by Hawileh et al., 2013 [23]

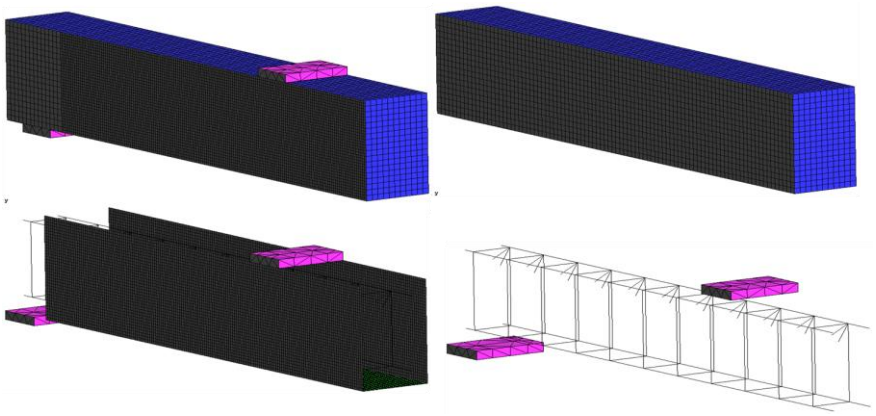

Figure 2. Geometry of RC beam, including every element and mesh

2.3.2 Material Properties

Materials can either be defined prior to assignment to the model or automatically applied to the finite elements generated on the corresponding geometric entities (e.g., concrete, steel plates, reinforcement, and CFRP shells). Each material type comes with default parameters, which can be modified to any desired, user-defined values. Table 1 summarizes the mechanical properties of the materials assigned to the various elements in the model. In GiD:

1. Concrete EC2-CC3DNonLinCementitious was the model name for the concrete. 2;
2. Elastic 3D-CC3DElastIsotropic was used to model the top and bottom plates;
3. Reinforcement EC2-CCReinforcement was used to model the longitudinal bar and tie reinforcements;
4. The CFRP sheet, which was strengthened with carbon fiber and epoxy, was modeled using the Shell-CCShellMaterial option;
5. An interface element was employed to represent the epoxy.

Table 1: Mechanical properties of the materials used in the finite element model (FEM).

Material	f'_{co} (MPa)	f_t (MPa)	f_y (MPa)	E (GPa)	Poisson's ratio
Concrete	54	4.55	-	34.5	0.2
Steel plates	-	-	-	200*	0.3*
Ties	-	-	600	202	0.3
Bars	-	-	611	202	0.3
1 layer CFRP	-	2800	-	160	0.3
Epoxy	-	30	-	10	0.3

* Default software value.

2.3.3 Material Models

The software provides a range of material models for various materials and applications, the majority of which are for reinforcement and concrete. The models consider both tensile and compressive behaviour, ATENA theory manual part 1 [24].

2.3.3.1 Concrete

ATENA provides a fracture-plastic constitutive model, which combines plasticity and fracture, for brittle materials such as concrete. The software employs a three-dimensional solid brick element with 8–20 nodes for concrete modeling

(see Figure 3). These isoparametric elements are integrated at interpolation points using Gauss integration. Each element node has three degrees of freedom (DoFs). This type of element enables the consideration of:

- Non-linear material properties;
- Plastic deformation and crushing, and;
- Cracking along three orthogonal directions.

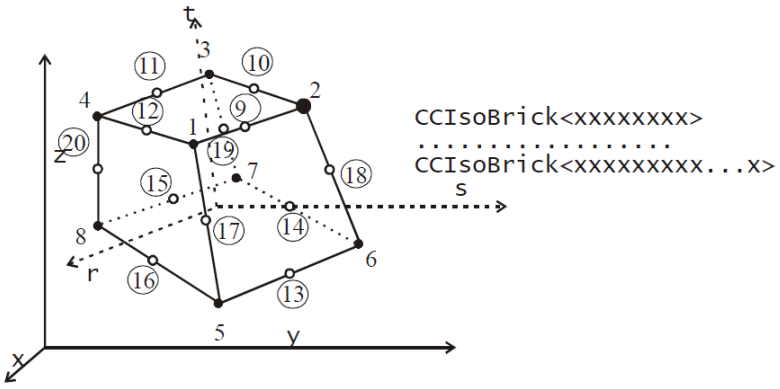

Figure 3. Geometry of Brick elements, ATENA theory manual part 1 [25]

Concrete is known to have microcracks between coarser aggregates and mortar even before loads are applied. These arise as a result of the mortar's segregation, shrinkage, and differential thermal expansion, as well as the stiffness difference between the mortar and the coarse aggregates. As a result, the tensile strength of concrete is poor. Since compressive strength may be increased by design, this is the most important factor.

Concrete shows nonlinear behavior when under uniaxial load. In ATENA, the non-linear behavior of concrete is represented using an effective stress, σ_c^{ef}, and an equivalent uniaxial strain, ε^{eq}. A typical stress–strain relationship is illustrated in

Figure 4. The effective stress, σ_c^{ef}, is assumed to coincide with the principal stress. At the same time, the equivalent uniaxial strain, ε^{eq}, corresponds to the principal strain and is introduced to bypass the need for considering Poisson's effect.

The ascending branch of the concrete stress–strain curve in compression was adapted from Equation 1, as recommended by the CEB-FIP Model Code [26] (see Figure 5). This equation applies to both normal-strength concrete (NSC) and high-strength concrete (HSC), providing a wide range of stress–strain curves from nearly linear to highly curved.

$$\sigma_c{}^{ef} = f'^{ef}{}_c = \frac{kx - x^2}{1 + (k-2)x} \quad where\ x = \frac{\varepsilon}{\varepsilon_c}\ \ and\ k = \frac{E_o}{E_c} \tag{1}$$

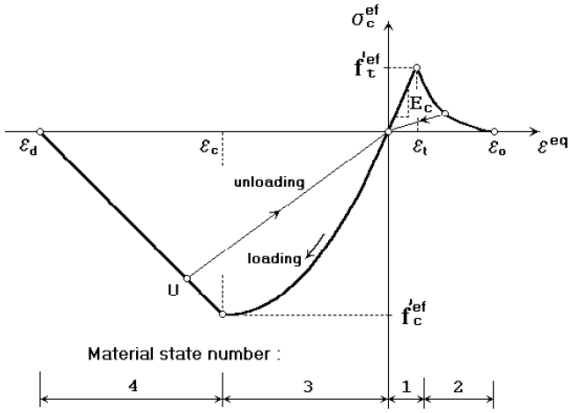

Figure 4. Uniaxial stress-strain law for concrete, ATENA theory manual part 1 [25]

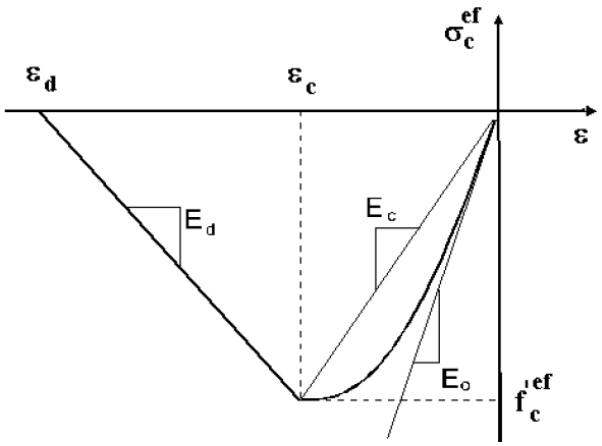

Figure 5. Compressive stress–strain diagram illustrating concrete behavior in compression (ATENA Theory Manual, Part 1 [25]

2.3.3.2 Steel Reinforcement

Both discrete and smeared reinforcement modeling approaches can be adopted in finite element simulations. In this study, the reinforcement cage was represented discretely, with individual bars modeled as one-dimensional reinforcing elements, whereas in ATENA, the bars were specifically simulated using three-dimensional truss elements. All reinforcing components were assumed to follow an elastic–perfectly plastic behavior.

As illustrated in Figure 6, a bilinear stress–strain relationship was assigned to the reinforcement, applicable for both smeared and discrete representations. The initial linear branch corresponds to the elastic modulus of steel, whereas the horizontal branch defines the yield plateau. Strain hardening was not included, as the adopted bilinear model sufficiently characterizes the behavior of the reinforcing steel used in the tested specimens.

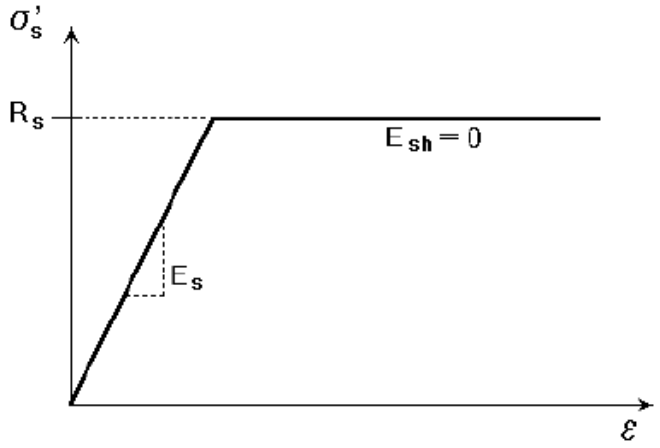

Figure 6. Bilinear stress–strain relationship for reinforcement (ATENA Theory Manual, Part 1) [25]

2.3.3.3 CFRP

ATENA-GiD can be used to simulate CFRP for confining beams, allowing fiber directions to be set in any direction. The fiber was assumed to be in the transverse direction alone in the modeling described in this chapter. Figure 7 illustrates how 3-D shell 20-node isoparametric brick elements (Ahmad shell elements) were used to simulate the CFRP fiber as distinct bars inside a thin layer of epoxy. The discrete bars, or CFRP fibers, in the brick elements can be found using a facility in GiD. In planes normal to the element's mid-surface, each node of an element has five degrees of freedom (three displacements and two rotations). Thin shell, thick shell, and even plate constructions can be modeled with this element. Figure 8 illustrates the four steps of the reinforcement multi-linear law in ATENA-GiD: elastic state,

yield plateau, hardening, and fracture. However, because CFRP behavior is elastic up to the point of rupture, this law was only characterized by three points in this study.

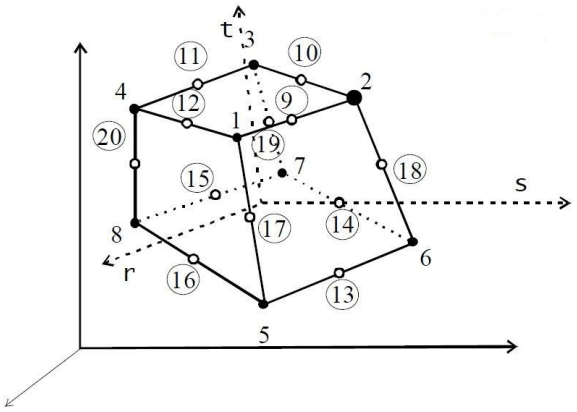

Figure 7. Geometry and the element's nodes (geometry of the FRP), ATENA theory manual part 1 [25]

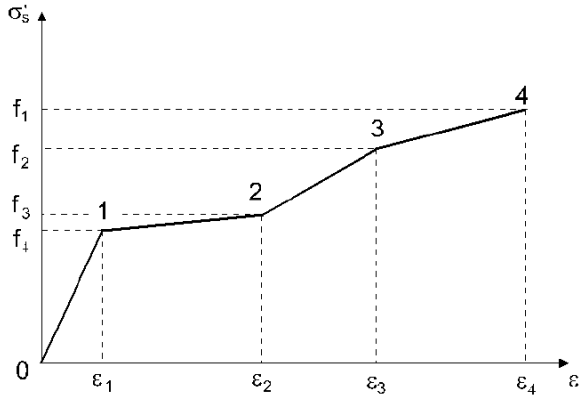

Figure 8. The multi-linear stress-strain law for reinforcement, ATENA theory manual part 1 [25]

2.3.4 Boundary Conditions

In ATENA-GiD, boundary conditions define supports, loads, displacements, monitoring points, symmetry constraints, missing contacts (e.g., master–slave), and element activity states. Intervals are used in GiD to determine the loads and boundary conditions. A set of loads and boundary conditions applied in a predetermined number of steps is represented by an interval. A comprehensive loading history can be specified using a suitable specification of intervals.

2.3.4.1 Support

The bottom surface of the steel plate attached to the tested beam was considered fully clamped (fixed), with zero displacement and rotation at all nodes along z = 0. In GiD, this is achieved by constraining the XYZ directions at the support points to prevent both vertical and lateral movements. In other words, all six degrees of freedom of this surface were fully restricted.

2.3.4.2 Displacement

A user-defined displacement increment was applied in the axial direction to the top surface of the steel plate attached to the concrete core (z = h). To replicate the behavior of the testing machine during RC beam loading, both before and after heating, these prescribed Z-direction displacements were applied to the top face of the rigid loading plate. The load was introduced in multiple sub-steps, allowing the axial pressure to increase gradually from zero (approximately –0.1 mm in GiD) to a predetermined final load, continuing until failure of the unwrapped or CFRP-wrapped beam. As a result, the top of the RC beam was constrained to move uniformly in the vertical direction while being restricted against lateral displacements in the X and Y directions.

2.3.4.3 Monitors

Establishing monitoring points is useful for tracking changes in specific quantities throughout the analysis. In other words, these points enable the observation of computational results during the simulation. At designated locations or surfaces, monitoring points can record the evolution of displacements (movement of a point), strains (relative deformation of an element), forces (stresses), or temperatures. Similar to strain gauges in experimental studies, monitoring points allow detailed tracking of specimen behavior. In this study, two monitoring points were placed at the middle bottom of each beam to measure axial (Z-direction) and lateral (Y-direction) displacements, while an additional monitor was used to calculate the load applied to the top steel plate.

2.3.4.4 Symmetry Condition

Regarding the beam and the top and bottom plates, it is believed that the YZ plane is a plane of symmetry. Applying a block to every displacement in the X direction—that is, perpendicular to the plane of symmetry—is how the software accomplishes this. To mimic this scenario, the rigid body rotations about the Z and Y axes at the plane of symmetry are likewise blocked. Except at the top and bottom nodes, displacements in the Z and Y dimensions are allowed.

2.3.4.5 Missing Contacts

It is important to note that GiD does not automatically detect potential contacts; therefore, master–slave contact conditions must be defined manually between volumes. The steel loading plates' top and bottom surfaces were constrained against lateral displacements, with the top face of the upper loading plate allowed to move uniformly in the vertical direction, while the bottom face of the lower plate was restricted in vertical movement. A fixed master–slave contact was applied at the interface between the top surface of the RC beam (slave) and the bottom surface of the top loading plate (master). Similarly, a fixed contact condition connected the top surface of the lower loading plate to the bottom surface of the RC beam.

Additionally, a master–slave boundary condition was applied between the CFRP shell and the concrete surface. This was implemented by connecting the two surfaces with a simple master–slave contact, using a thin shell volume that conformed to the concrete beam geometry to represent the concrete volume accurately.

2.3.4.6 Interval Data

GiD uses intervals (referred to as "interval data" in the application) to express the loading and temperature distribution histories. Increasing the load gradually until it fails could be the goal. Another interval with several vertical displacement steps is needed to simulate the loading of the RC beam to failure. Knowing the vertical displacement at failure of the tested RC beams helped determine the vertical steps. Every step represented a portion of the total displacement at failure.

2.3.4.7 Mesh Generation

The final phase of the pre-processing phase with GiD is the creation of a FE mesh. The speed, memory requirements, and quality of the analysis results are all significantly impacted by the FE mesh quality. In GiD, a structured brick (hexahedra) mesh was used to mesh the beams. Tetrahedral (linear elastic) elements were used to mesh the top and bottom steel plates, and quadratic hexahedral elements were used to structure the CFRP shell. The aspect ratio of the structured volume elements should be less than or equal to 3:1. To accomplish the master-slave idea, distinct element sizes must be assigned to the concrete beam volume (smaller elements) and the steel plate volumes (bigger elements). It is generally advised to assign a number of divisions for reinforcement (bars and ties); that is, the ATENA kernel divides the bars into elements at intersections with the surrounding elements. To prevent potential out-of-memory issues when using the ATENAStudio interface, it was found that selecting the "Non-quadratic element" option in GiD for all materials except the CFRP shells significantly reduced memory usage.

2.4 FE Non-linear Analysis

It should be noted that if geometry, materials, or boundary conditions change, the mesh needs to be created afresh before doing a non-linear analysis. Clicking on the Calculate command in the GiD interface will begin the FEA's execution. The software will then begin to generate the input files for each stage of the non-linear analysis. During non-linear analysis, various parameters can be monitored, including the applied load progression, beam displacements,

crack widths, and real-time visualization of results, allowing observation of deformation shapes and crack patterns as the analysis progresses. The interface displays several windows:

- Window A: Tracks steps and iterations;
- Window B: Displays important ATENA kernel messages throughout the analysis;
- Window C: Configures which results are presented;
- Window D: Shows the number of steps, iterations, and overall analysis progress;
- Window E: Provides a visual representation of the structure under analysis;
- Window F: Presents either a user-defined diagram or the default convergence plot.

2.5 Post-Processing

The generated model is then post-processed in the GiD or in the ATENAStudio after completing the non-linear FEA in the ATENAStudio interface and storing the modifications. GiD served as the post-processor for this project. Before the post-processing features for each step can be shown or chosen, the computed results in ATENAStudio must be imported into GiD. Figure 9 displays typical post-processing elements.

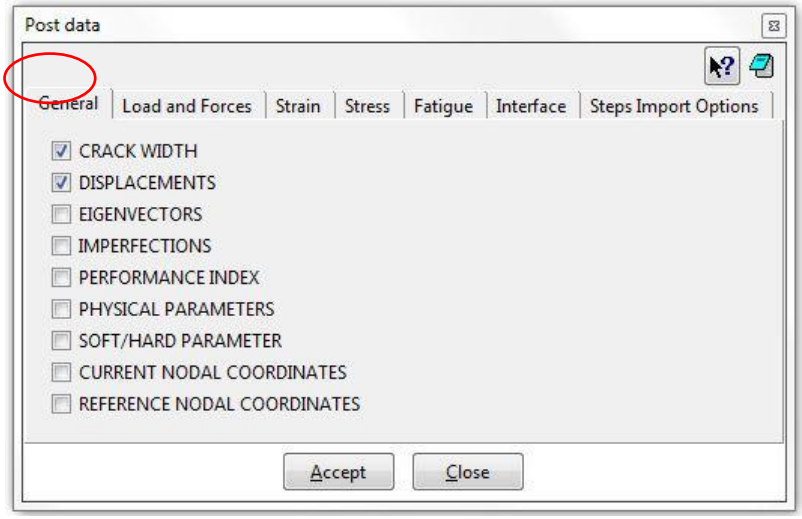

Figure 9. Selection of post-processing data

2.6 FE Modelling of RC Beams

As mentioned, previously, two scenarios were simulated:

- Control RC beams without CFRP reinforcement;
- RC beams strengthened with a single unidirectional CFRP sheet bonded to the exterior surface.

2.6.1 FE Modeling of the Control RC Beam

2.6.1.1 Model Development

The FE model for the control RC beam is referred to as the static analysis model throughout this study. Due to the beam's symmetry, only half of the beam was modeled, with the appropriate boundary conditions applied at the plane of symmetry. Experimental details of the modeled beam are provided in [23]. Relevant material properties are listed in Table 1, while additional information regarding beam dimensions and reinforcement details (e.g., diameter, length) can be found in

Figure 1 and 2. The finite element analysis yielded load versus localized displacement results, which were presented as load–deflection curves. These curves were subsequently compared with the experimental data reported in [23].

2.6.2 FE Modelling of CFRP-Applied RC Beam

2.6.2.1 Developing the Model

Another model for CFRP-applied RC beams with a single CFRP layer was created using the same FE model that was discussed in the previous section as a guide. Table 1 has already provided a description of the material qualities. The CFRP shells were incorporated into the model to assess the impact of strengthening, which is the primary distinction between this model and the one previously discussed.

3. Results and Discussion

The FE models were validated by comparing the predicted load–midspan deflection response and ultimate load capacity with the experimental measurements obtained for the tested RC beam specimens.

3.1 Verification of Finite Element Model: Control Beam

Figure 10 plots the experimental and FEA load-deflection curves for the control RC beams. Within ten percent of one another are the maximum load-bearing capacities. Reasonably accurate predictions were made for the deflection at maximum load. Regarding the beginning slope of the curves' rising portion, the FE curves and the experimental data also correspond quite well. The model seems to underestimate the final axial load, though. The stress-strain curves in FE and experiment both exhibit roughly bilinear behavior. Figure 11 displays a typical dislocation and crack pattern as predicted by the 3-D model, both before loading and upon failure.

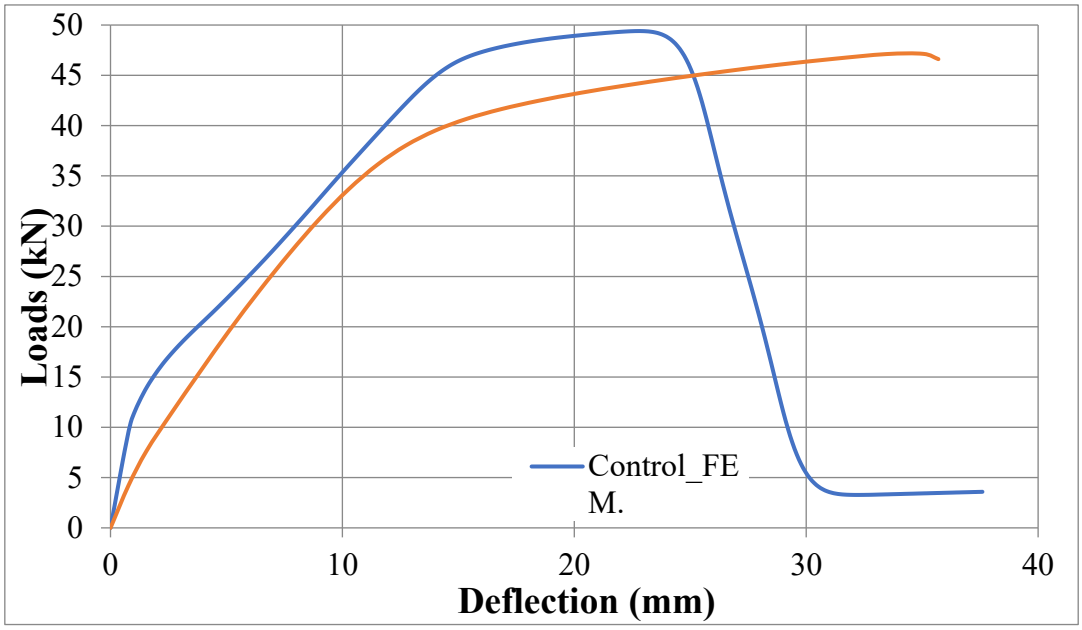

Figure 10. Experimental and FEA load-deflection curves for the control RC beam

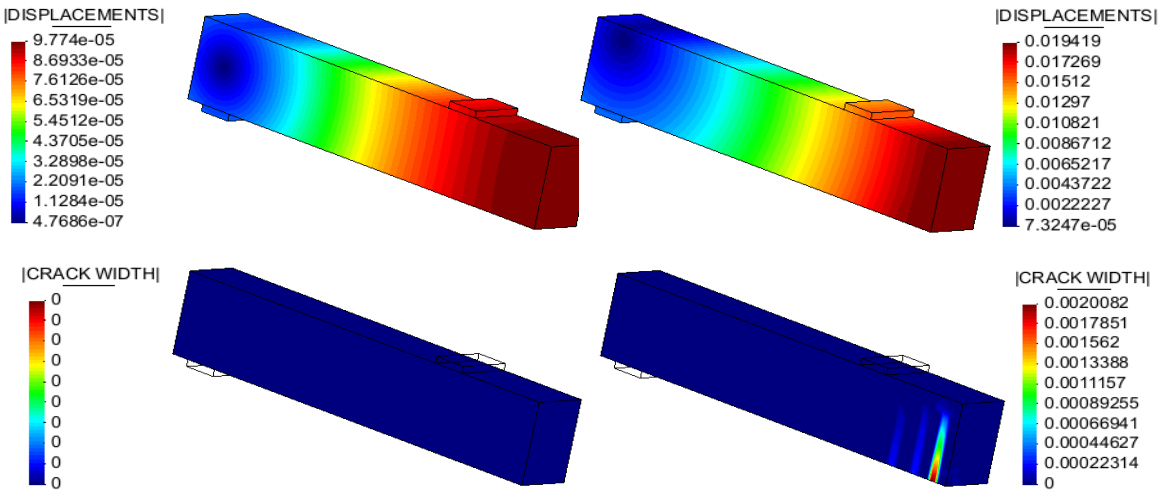

Figure 11. FEA displacements and crack widths in 3D control model

3..2 Verification of Finite Element Model: CFRP reinforced

Figure 12 plots the load-deflection curves produced by this model against those acquired empirically. The results show good agreement, with reasonable accuracy anticipated for both maximum loads and deflection. Once more, the experimental and FE load-deflection curves exhibit roughly bilinear behavior. Figure 13 displays a typical displacement and crack pattern both prior to loading and at failure.

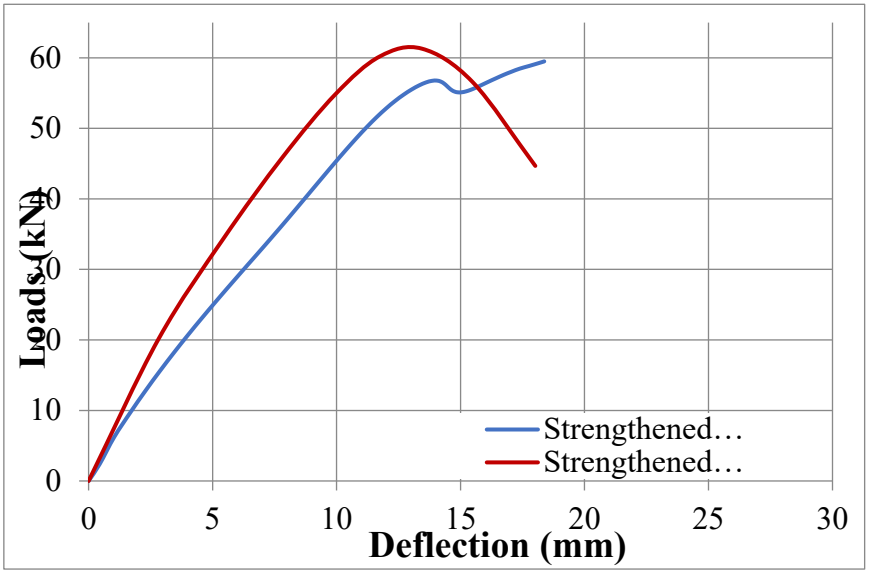

Figure 12. Experimental and FEA load-deflection curves for CFRP reinforced RC beam

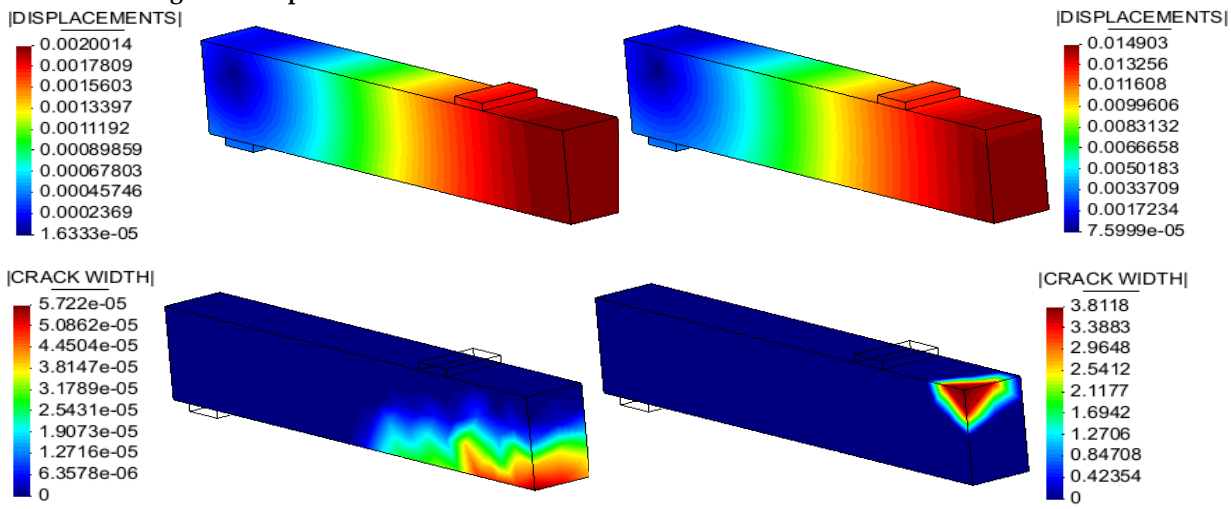

Figure 13. Experimental and FEA displacements and crack widths for CFRP reinforced RC beam

When comparing the experimental results from the taken research undertaken by Hawileh et al., 2013 [23] with FEM analysis shown in Figure 10 and Figure 12, it can be seen that the maximum load bearing capacity and deflection for the control beam was 47.7 kN and 24.5 mm, respectively, after rapping the beam with one unidirectional CFRP sheet as U-wraps, the load increased and deflection decreased by 24.9 % and 48.2 %, respectively. When using the same research for verification using FE software, the maximum load bearing capacity and deflection for the simulated model were 49.4 kN and 37.6 mm, respectively, after adding the CFRP sheet to the model, similar to that of the experimental specimen. After the analysis stage, the load increased and deflection decreased by 24.1 % and 52.1 %, respectively.

It's clear from Figure 10 and Figure 12 that there is a reasonable agreement between the experimentally measured and FE predicted load-midspan deflection results at all stages of loading till failure of the specimen, see Figure 14.

Overall, it can be stated that the created FE models are trustworthy and legitimate, and they could be a useful numerical tool for examining the performance of RC beams reinforced with CFRP fabrics.

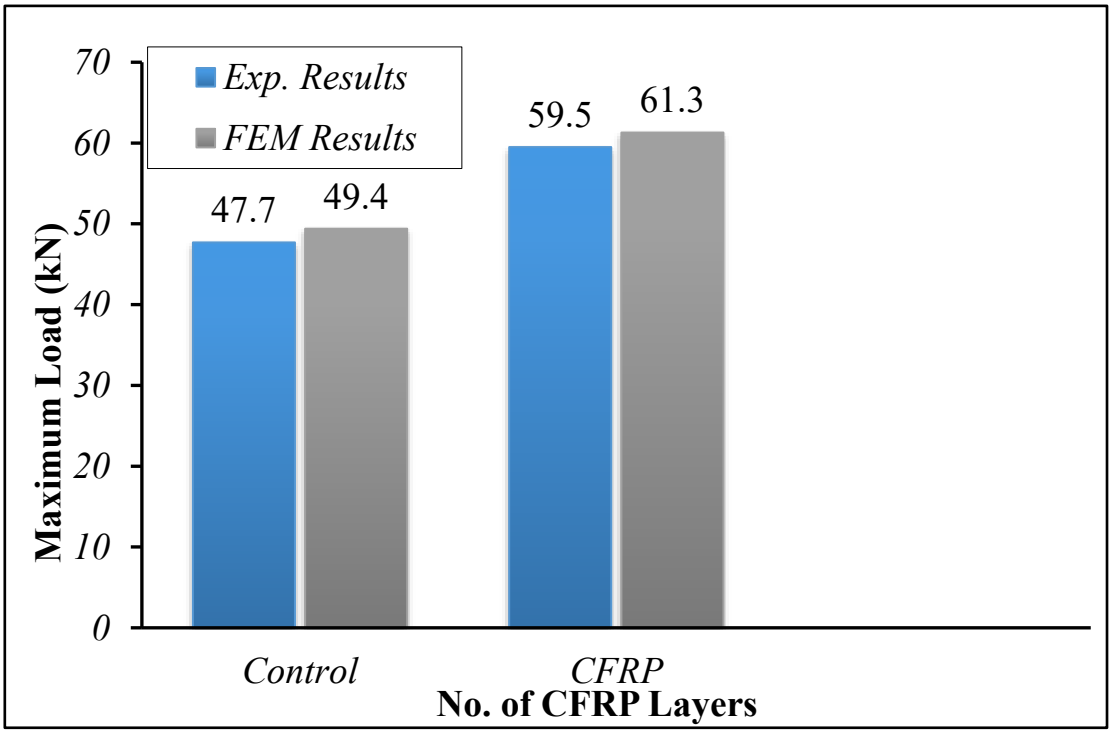

Figure 14. Experimental and FEA load-bearing capacity comparison

4. Conclusions

The key findings of this study can be summarized as follows:

1- The overall behavior of the FE models, as represented by the load–deflection curves, aligns closely with the experimental results obtained from the tested RC beams;

2- Non-linear FEA effectively predicts the performance of FRP-retrofitted beams, accurately capturing load–deformation behavior, ultimate load capacity, and the cracking process in a manner consistent with experimental observations;

3- Strengthening concrete beams with CFRP fabrics reduces deflections and enhances load-carrying capacity, while the resulting cracks are smaller and more uniformly distributed;

4- The ultimate load-carrying capacity of beams can be doubled by using a proper combination of horizontal and vertical fibers coupled with the proper epoxy;

5- ATENA-GiD software seems to be very effective for simulating both control and CFRP reinforced beams. This is a unique software that can be used only for RC elements;

6- Applying CFRP sheets to both the bottom and sides of the beam enhances structural performance compared to using CFRP only on the bottom surface;

7- All CFRP-strengthened beams displayed brittle behavior, indicating the need for a higher safety factor in design considerations.

Based on the outcomes of this study, further research is recommended to better understand the complex behavior of CFRP materials and CFRP-strengthened concrete elements:

1. Strengthening RC beams with CFRP fabrics under eccentric loading conditions;
2. Reinforcing RC beams subjected to sustained loads; while steel bars were employed in this study, FRP bars could be considered as a corrosion-resistant alternative, accounting for thermal effects during heating and cooling;
3. Strengthening full-scale RC square or rectangular beams;
4. Investigating the repair of HSC beams with CFRP, as this study focused on moderately high-strength concrete.

Author Contributions: Conceptualization, Yaman Al-Kamaki, Riadh Al-Mahaidi, and Razaq Ferhadi; methodology, Yaman Al-Kamaki and Razaq Ferhadi; software, Yaman Al-Kamaki; validation, Yaman Al-Kamaki, Riadh Al-Mahaidi, Mand Kamal Askar, and Razaq Ferhadi; formal analysis, Yaman Al-Kamaki and Razaq Ferhadi; investigation, Yaman Al-Kamaki and Razaq Ferhadi; resources, Mand Kamal Askar and Razaq Ferhadi; data curation, Yaman Al-Kamaki; writing original draft preparation, Yaman Al-Kamaki and Razaq Ferhadi; writing review and editing, Riadh Al-Mahaidi, Mand Kamal Askar, and Razaq Ferhadi; visualization, Yaman Al-Kamaki and Razaq Ferhadi; supervision, Riadh Al-Mahaidi and Razaq Ferhadi; project administration, Yaman Al-Kamaki and Razaq Ferhadi; funding acquisition, Riadh Al-Mahaidi and Razaq Ferhadi.

Funding: This research received no external funding.

Data Availability Statement: The data that support the findings of this study are available from the corresponding author upon reasonable request.

Acknowledgments: The authors would like to thank the following undergraduate students for their interest in this work, which may serve as a valuable reference for their final year projects: Zanko Abdullah Hussein, Awder Esmael Mawlud, Dilovan Idrees Majeed, and Rekar Karim Ahmed. Their engagement and enthusiasm are greatly appreciated.

Conflicts of Interest: The authors declare no conflicts of interest.

Abbreviations

The following abbreviations are used in this manuscript:

ATENA	**Advanced Tool for Engineering Nonlinear Analysis**
CFRP	**Carbon Fiber Reinforced Polymer**
FEA	**Finite Element Analysis**
FEM	**Finite Element Method or Modeling**
FRPs	**Fibre Reinforced Polymers**
GFRP	**Glass Fiber Reinforced Polymer**
GiD	**Graphic Interface Device**
RCB	**Reinforced Concrete Beam**
NSC	**Normal Strength Concrete**
HSC	**High Strength Concrete**

References

1. W. WENWEI and L. GUO, "Experimental study and analysis of RC beams strengthened with CFRP laminates under sustaining load," International Journal of Solids and Structures, vol. 43, no. 6, pp. 1372-1387, 2006/03/01/ 2006, doi: https://doi.org/10.1016/j.ijsolstr.2005.03.076.
2. A. AL-YOUSUF et al., "The Behavior of Reinforced Concrete Slabs Strengthened by Different Patterns and Percentages of Carbon Fiber-Reinforced Polymer (CFRP) Plate," Construction Materials, vol. 5, no. 2, p. 24, 2025. [Online]. Available: https://www.mdpi.com/2673-7108/5/2/24.
3. Y. GHERNOUTI, B. RABEHI, A. BENHAMNA, and A. HADJ MOSTEFA, "Strengthening of concrete beams by CFRP: Experimental study and finite element analysis," Journal of Building Materials and Structures, vol. 1, no. 2, pp. 47-57, 2014.
4. H. SINGHAL, "Finite Element Modeling of Retrofitted RC Beams," 2009.
5. C. BEDON, "Review on the use of FRP composites for facades and building skins," American Journal of Engineering and Applied Sciences, vol. 9, no. 3, pp. 713-723, 2016.
6. N. ARAVIND, A. K. SAMANTA, J. V. THANIKAL, and D. K. SINGHA ROY, "An experimental study on the effectiveness of externally bonded corrugated GFRP laminates for flexural cracks of RC beams," Construction and Building Materials, vol. 136, pp. 348-360, 2017/04/01/ 2017, doi: https://doi.org/10.1016/j.conbuildmat.2017.01.047.
7. Z. YAO, "Nonlinear finite element analysis of reinforced concrete beams," HKU Theses Online (HKUTO), 2013.
8. J. V. FRANK, "Nonlinear Finite Element Analysis of Reinforced Concrete Membranes," ACI Structural Journal, vol. 86, no. 1, 1/1/1989, doi: 10.14359/2620.

9. R. STRAMANDINOLI and H. L. ROVERE, "Finite element model for nonlinear analysis of reinforced concrete beams and plane frames," Revista IBRACON de Estruturas e Materiais, vol. 10, pp. 386-414, 2017.
10. M. CRISFIELD, "Finite elements in plasticity—theory and practice, DRJ Owen and E. Hinton, Pineridge Press, Swansea," ed: Wiley Online Library, 1981.
11. K. R. RAJAGOPAL, NONLINEAR ANALYSIS OF REINFORCED CONCRETE BEAMS, BEAM-COLUMNS AND SLABS BY FINITE ELEMENTS. Iowa State University, 1976.
12. C. JEYAMOHAN, "Non-linear finite element of analysis of reinforced concrete members," 1987.
13. D. NGO and A. C. SCORDELIS, "Finite element analysis of reinforced concrete beams," in Journal Proceedings, 1967, vol. 64, no. 3, pp. 152-163.
14. A. H. NILSON, "Nonlinear analysis of reinforced concrete by the finite element method," in Journal Proceedings, 1968, vol. 65, no. 9, pp. 757-766.
15. D. DUTHINH and M. A. STARNES, "Strengthening of reinforced concrete beams with carbon FRP," 2001.
16. Z. J. YANG, J. F. CHEN, and D. PROVERBS, "Finite element modelling of concrete cover separation failure in FRP plated RC beams," Construction and Building Materials, vol. 17, no. 1, pp. 3-13, 2003/02/01/ 2003, doi: https://doi.org/10.1016/S0950-0618(02)00090-9.
17. T. SUPAVIRIYAKIT, P. PORNPONGSAROJ, and A. PIMANMAS, "Finite element analysis of FRP-strengthened RC beams," Songklanakarin J. Sci. Technol, vol. 26, no. 4, pp. 497-507, 2004.
18. R. SANTHAKUMAR, E. CHANDRASEKARAN, and R. DHANARAJ, "Analysis of retrofitted reinforced concrete shear beams using carbon fiber composites," Electronic journal of structural engineering, vol. 4, pp. 66-74, 2004.
19. B. FERRACUTI, M. SAVOIA, and C. MAZZOTTI, "A numerical model for FRP–concrete delamination," Composites Part B: Engineering, vol. 37, no. 4, pp. 356-364, 2006/06/01/ 2006, doi: https://doi.org/10.1016/j.compositesb.2005.08.002.
20. B. GAO, C. K. Y. LEUNG, and J.-K. KIM, "Failure diagrams of FRP strengthened RC beams," Composite Structures, vol. 77, no. 4, pp. 493-508, 2007/02/01/ 2007, doi: https://doi.org/10.1016/j.compstruct.2005.08.003.
21. V. CERVENKA, L. JENDELE, and J. CERVENKA, "ATENA program documentation," Theory and User Manual, Cervenka Consulting, Prague, 2008.
22. V. ČERVENKA, J. ČERVENKA, Z. JANDA, and D. PRYL, "ATENA Program Documentation Part 8 User's Manual for ATENA GiD Interface," Červenka Consulting, sro, Prague, 2019.
23. R. A. HAWILEH, M. Z. NASER, and J. A. ABDALLA, "Finite element simulation of reinforced concrete beams externally strengthened with short-length CFRP plates," Composites Part B: Engineering, vol. 45, no. 1, pp. 1722-1730, 2013/02/01/ 2013, doi: https://doi.org/10.1016/j.compositesb.2012.09.032.
24. V. CERVENKA, L. JENDELE, and J. CERVENKA, ATENA Program Documentation Part 1, ATENA theory manual. Prague, Czech Republic: Cervenka Consulting, 2012.
25. V. ČERVENKA, L. JENDELE, and J. ČERVENKA, "ATENA program documentation–Part 1," Cervenka Consulting sro, 2021.
26. M. CEB-FIP, "90, Design of concrete structures. CEB-FIP Model Code 1990," British Standard Institution, London, 1993.